EAST EUROPEAN JOURNAL OF PHYSICS. 1. 396-400 (2026)
DOI:10.26565/2312-4334-2026-1-47 ISSN 2312-4334

ROOM-TEMPERATURE FERROMAGNETISM AND SPIN POLARIZATION IN SILICON DOPED WITH MANGANESE

Olmas E. Sattarov*, Bahromjon A. Abdurakhmanov, Giyos A. Kushiev, Stanislav A. Tachilin, Temur B. Ismailov, Zabarjat N. Umarxodjayeva
Tashkent state technical university, Uzbekistan, 100095, Tashkent, University St., 2
**Corresponding Author e-mail: ismaylovb81@gmail.com*

Received December 5, 2025; revised February 18, 2026; accepted February 23, 2026

In this study, we investigate the magnetic properties of silicon doped with manganese via thermal diffusion. The results demonstrate clear evidence of room-temperature ferromagnetism in p-type Si, arising from the spin alignment of Mn atoms and hole-mediated conductivity. Magnetoresistance and hysteresis analyses confirm spin-dependent transport, indicating that carrier-mediated exchange interactions are responsible for the observed magnetic ordering. The combination of atomic force microscopy (AFM), scanning electron microscopy (SEM), and energy-dispersive X-ray spectroscopy (EDS) confirms the successful incorporation of Mn atoms into the Si lattice without evidence of large secondary precipitates. The hysteresis loops measured at both 150 K and 300 K for the sample processed at T = 1050 °C ($\rho = 4.2\times10^3$ Ω·cm) reveal stable ferromagnetic behavior, with coercive fields of 115 Oe and 87 Oe, respectively. These findings open promising perspectives for the development of silicon-based spintronic devices using CMOS-compatible thermal-diffusion technology.

Keywords: *Silicon; Manganese diffusion; Ferromagnetism; Nanoclusters; Hysteresis; Spintronics*
PACS: 78.30.Am

INTRODUCTION

Ferromagnetism in semiconductors has attracted growing attention due to its potential for realizing next-generation spintronic devices that combine charge and spin degrees of freedom. Silicon, as the cornerstone of modern microelectronics, is particularly appealing for spintronics because of its well-established processing technology, long spin-coherence length, and excellent compatibility with CMOS fabrication. However, pristine silicon is intrinsically nonmagnetic, and achieving ferromagnetic ordering within Si remains a challenging task.

One of the most promising approaches to induce magnetism in Si involves doping with 3d transition metals, such as manganese (Mn), which introduces localized magnetic moments [1–4]. When properly incorporated into the Si lattice, Mn atoms can interact with charge carriers via exchange coupling, resulting in carrier-mediated ferromagnetism. This phenomenon has been extensively studied in III–V diluted magnetic semiconductors [5–9], whereas its realization in Si is often limited by solubility constraints and the tendency toward phase segregation.

MATERIALS AND METHODS

Several methods have been explored to introduce Mn into silicon, including ion implantation [10–13], molecular beam epitaxy (MBE), and chemical vapor deposition (CVD). While these techniques have demonstrated partial success, they often lead to crystal damage, clustering, or the formation of secondary Mn-silicide phases. In contrast, thermal diffusion represents a technologically compatible and less destructive alternative that allows controlled incorporation of Mn atoms into the Si lattice while largely preserving the host crystal structure [14–16].

In this work, we investigate boron-doped p-type silicon subjected to manganese thermal diffusion in the temperature range of 1000–1150°C. Particular attention is paid to the sample processed at T = 1050 °C, which exhibits a resistivity of $\rho = 4.2\times10^3$ Ω·cm and shows the most stable ferromagnetic response.

Before diffusion, the Si wafers underwent a standard RCA cleaning procedure. AFM inspection of reference (undoped, untreated) Si wafers showed a smooth surface with low roughness, indicating the absence of significant surface features prior to Mn incorporation. After diffusion, the samples were subjected to identical mechanical and chemical surface treatments, including gentle chemical cleaning, to remove any residual surface contaminants or unreacted Mn species. Such cleaning may slightly affect the very topmost surface layer; however, the main morphological and compositional features observed by AFM and EDS are attributed to the near-surface diffusion region rather than to removable surface residues.

Electrical transport parameters (resistivity ρ, carrier concentration, and mobility) were measured using the Hall effect in Van der Pauw geometry. The data for the full series of diffusion temperatures are summarized in Table 1. Among these, the sample diffused at 1050 °C ($\rho = 4.2\times10^3$ Ω·cm) was selected for detailed structural and magnetic analysis presented below.

It should be noted that AFM and EDS are surface- and near-surface-sensitive techniques, probing only the top tens to hundreds of nanometers. Therefore, information about the bulk is obtained indirectly from magnetic and transport measurements, which reflect the averaged properties of the entire diffusion layer.

Cite as: O.E. Sattarov, B.A. Abdurakhmanov, G.A. Kushiev, S.A. Tachilin, T.B. Ismailov, Z.N. Umarxodjayeva, East Eur. J. Phys. 1, 396 (2026), https://doi.org/10.26565/2312-4334-2026-1-47

Table 1. Electrical parameters of boron-doped silicon after manganese thermal diffusion

no.	Diffusion temperature (°C)	Mobility of current carriers μ, cm^2/V·s	Resistivity ρ (Ω·cm)	Carrier concentration p or n (cm^{-3})	Conductivity type
1.	T=1000 ^{0}C	205	$4.9\cdot10^2$	$6.22\cdot10^{13}$	*p*
2.	T=1025 ^{0}C	198	$1.1\cdot10^3$	$2.86\cdot10^{13}$	*p*
3.	T=1050 ^{0}C	231	$4.2\cdot10^3$	$6.44\cdot10^{12}$	*p*
4.	T=1075 ^{0}C	196	$8.3\cdot10^4$	$3.84\cdot10^{11}$	*p*
5.	T=1100 ^{0}C	1165	$1.07\cdot10^3$	$5.01\cdot10^{12}$	*n*
6.	T=1150 ^{0}C	1205	$6.2\cdot10^2$	$8.36\cdot10^{14}$	*n*

RESULTS

High-purity single-crystalline boron-doped p-type silicon (Si:B) wafers with an initial resistivity of 10 Ω·cm (KDB-10 grade) were used as the starting material. Manganese incorporation was carried out by thermal diffusion from the gas phase in evacuated quartz ampoules. The diffusion temperature was varied between 1000 °C and 1150 °C with a fixed annealing time of 60 minutes, followed by cooling to room temperature under vacuum.

Hall measurements confirmed that changing the diffusion temperature allows control over carrier compensation, leading to compensated, strongly compensated, or overcompensated samples (Table 1). The present structural and magnetic analysis focuses on the sample processed at T = 1050 °C, which exhibits $\rho = 4.2\times10^3$ Ω·cm and p-type conductivity.

DISCUSSION

Figure 1 shows a three-dimensional AFM topography of the Si surface after Mn diffusion at 1050 °C. The scan area of 5.0×5.0 μm² reveals pronounced nanoscale surface modulation. Compared to the smooth surface of the reference Si wafer before diffusion, the treated sample exhibits clear corrugation and localized features, indicating structural and electronic inhomogeneities induced by Mn incorporation.

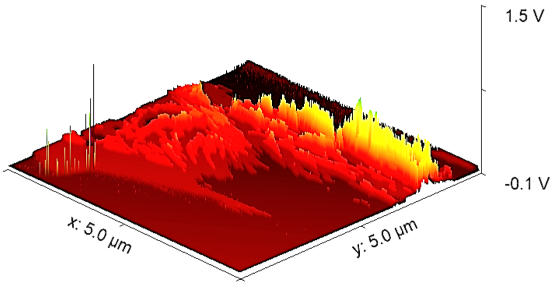

Figure 1. 3D AFM topography of the Si surface after Mn diffusion. The scan area is 5.0×5.0 μm², revealing nanoscale surface fluctuations associated with Mn-induced clusters. The sample has a resistivity of $\rho = 4.2\times10^3$ Ω·cm and was processed at T = 1050°C

The bright elevated regions are interpreted as morphological features formed during high-temperature Mn diffusion. While these features may be associated with local dopant redistribution, AFM alone does not allow direct determination of their chemical composition. This morphology is consistent with possible partial redistribution or aggregation of Mn atoms during diffusion. However, AFM provides purely topographical information and does not directly reveal magnetic inhomogeneities. Such structural inhomogeneities may influence the magnetic behavior observed in SQUID measurements; however, direct evidence of exchange interactions is derived from magnetometry data rather than from AFM observations.

Energy-dispersive X-ray spectroscopy (EDS) performed in SEM mode confirmed the presence of Mn in the near-surface region (Figure 2), within the detection limits of the technique. Distinct Mn–L and Mn–K peaks were observed together with the dominant Si–K line. Minor C and O signals are attributed to surface contamination and native oxide. The nanoscale surface features observed by AFM (tens of nanometers) are substantially smaller than the effective compositional averaging volume of EDS. Therefore, possible local compositional fluctuations at the nanometer scale cannot be resolved by SEM-EDS. The apparent uniformity of Mn distribution at the micrometer scale does not contradict the presence of nanoscale morphological variations. No distinct compositional signatures characteristic of extended Mn–silicide secondary phases were detected within the sensitivity limits of SEM-EDS. While EDS is inherently surface-sensitive, the absence of strong signals from secondary phases suggests that the crystal structure is largely preserved in the diffusion region.

Magnetization measurements were carried out using a superconducting quantum interference device (SQUID) in the temperature range from 150 K to 300 K for the sample diffused at 1050 °C. Figure 3 shows the hysteresis loop measured at 150 K, demonstrating clear ferromagnetic behavior with a coercive field H_c = 115 Oe, remanent magnetization $M_r = 8\times10^{-5}$ emu/cm^3, and saturation magnetization $Ms = 2\times10^{-4}$ emu/cm^3.

At room temperature (300 K), the same sample retains ferromagnetic behavior (Figure 4), with slightly reduced parameters: $Ms = 1.6\times10^{-4}$ emu/cm^3, $Mr = 3.5\times10^{-5}$ emu/cm^3, and Hc = 87 Oe. The decrease in magnetization with increasing temperature is attributed to thermal spin disorder and weakening of exchange coupling among Mn moments. Nevertheless, the persistence of a hysteresis loop at 300 K confirms the existence of stable room-temperature ferromagnetism.

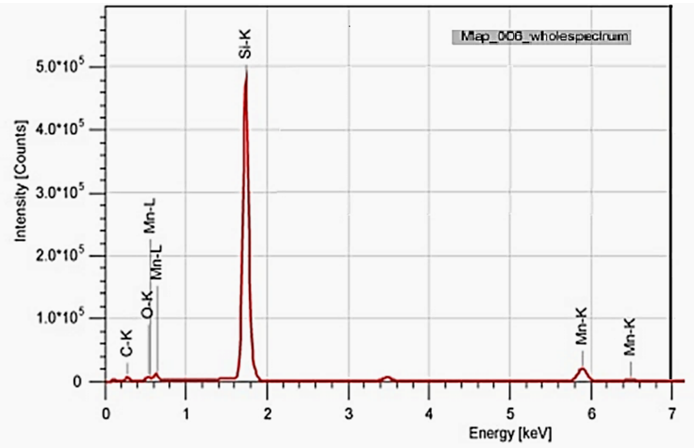

Figure 2. EDS spectrum of Mn-diffused silicon showing Mn–L and Mn–K peaks, confirming dopant incorporation. The sample has a resistivity of ρ = 4.2 × 10³ Ω·cm and was processed at T = 1050°C

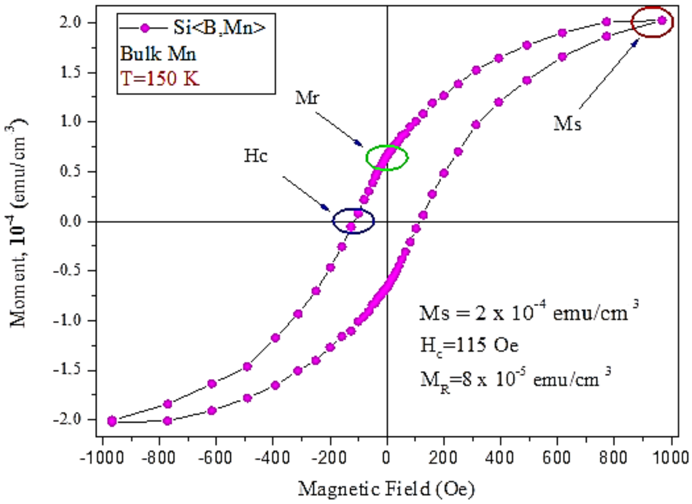

Figure 3. Magnetic hysteresis loop of Mn- and B-doped silicon (Si<B,Mn>) measured at 150 K, demonstrating clear ferromagnetic behavior (Ms = 2 × 10^{-4} emu/cm³, Mr = 8 × 10^{-5} emu/cm³, Hc = 115 Oe). The sample has a resistivity of ρ = 4.2 × 10³ Ω·cm and was processed at T = 1050 °C.

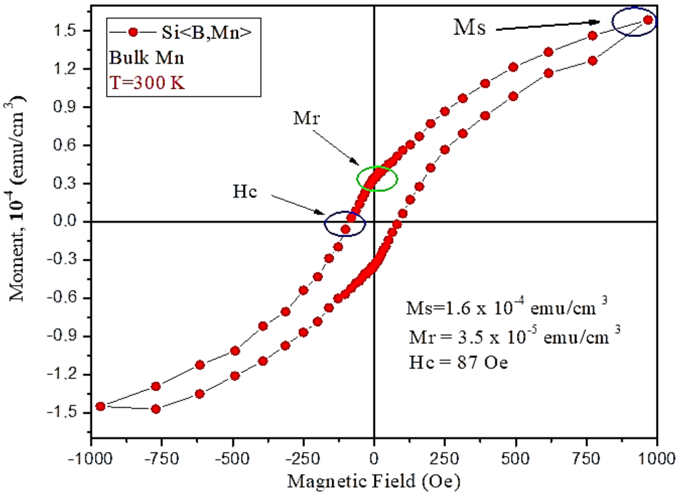

Figure 4. Magnetic hysteresis loop of Mn- and B-doped silicon (Si<B,Mn>) measured at 300 K, showing stable room-temperature ferromagnetism (Ms = 1.6×10^{-4} emu/cm³, Mr = 3.5×10^{-5} emu/cm³, Hc = 87 Oe). The sample has a resistivity of ρ = 4.2×10³ Ω·cm and was processed at T = 1050 °C.

The observed behavior is consistent with the model of carrier-mediated ferromagnetism in diluted magnetic semiconductors [17]. In the present system, hole-mediated exchange interactions between localized Mn moments, enhanced by boron co-doping, are responsible for spin alignment. At higher diffusion temperatures (>1075 °C), increased clustering and changes in carrier type (Table 1) suggest that excessive Mn aggregation may reduce long-range magnetic ordering. Although detailed magnetic data are shown here for the 1050 °C sample, the overall trend indicates that this temperature range provides an optimal balance between Mn incorporation and structural preservation.

Compared to ion implantation [18–20], thermal diffusion offers a less destructive and more CMOS-compatible route, ensuring better crystalline preservation and more uniform dopant incorporation—both crucial for silicon-based spintronic platforms.

Manganese diffusion in boron-doped silicon appears to promote ferromagnetic ordering at room temperature while largely preserving the structural integrity of the silicon lattice. The observed interplay between microstructure, charge carrier type, and magnetic behavior suggests that controlled Mn diffusion may provide a feasible pathway toward the development of spin-polarized silicon-based materials [21–25].

CONCLUSIONS

The structural, compositional, and magnetic properties of manganese-diffused boron-doped silicon were investigated, with detailed analysis focused on the sample processed at T = 1050 °C ($\rho = 4.2 \times 10^3\ \Omega\cdot\text{cm}$). AFM revealed the formation of nanoscale surface corrugations and Mn-rich clusters compared to the smooth reference Si surface before diffusion. SEM/EDS confirmed the presence and near-surface distribution of Mn without evidence of large secondary precipitates, suggesting that the crystal structure is largely preserved in the diffusion layer.

Magnetic measurements demonstrated clear ferromagnetic behavior at both 150 K and room temperature, with well-defined hysteresis loops. The observed room-temperature ferromagnetism is attributed primarily to carrier-mediated exchange interactions between localized Mn moments and holes introduced by boron co-doping, while nanoscale Mn-rich regions may contribute to local magnetic ordering. These results establish that controlled Mn thermal diffusion in boron-doped silicon is a viable route toward realizing room-temperature ferromagnetic semiconductors compatible with existing silicon technologies and promising for future spintronic applications.

ORCID

Olmas E. Sattarov, https://orcid.org/0009-0008-9121-3541, **Bahromjon A. Abdurakhmanov,** https://orcid.org/0009-0009-8424-4267, **Giyos A. Kushiev,** https://orcid.org/0009-0006-5847-6601, **Stanislav A. Tachilin,** https://orcid.org/0009-0007-3923-2131, **Temur B. Ismailov,** https://orcid.org/0000-0001-5179-3168, **Zabarjat N. Umarxodjayeva,** https://orcid.org/0009-0000-1488-6410

REFERENCES

[1] T. Dietl, and H. Ohno, "Dilute ferromagnetic semiconductors: Physics and spintronic structures," Reviews of Modern Physics, **86**, 187 (2014). https://doi.org/10.1103/RevModPhys.86.187

[2] J. Schmalhorst, D. Ebke, and A. Weddemann, "On the influence of bandstructure on transport properties of magnetic tunnel junctions with $Co_2Mn_{1-x}Fe_xSi$ single and multilayer electrode," Journal of Applied Physics, **104**, 043919 (2008). https://doi.org/10.1063/1.2973664

[3] B.A. Aronzon, V.V. Rylkov, S.N. Nikolaev, V.V. Tugushev, S. Caprara, and V.V. Podolskii, "Room-temperature ferromagnetism and anomalous Hall effect in $Si_{1-x}Mn_x$ ($x \approx 0.35$) alloys," Physical Review B, **84**, 075209 (2011). https://doi.org/10.1103/PhysRevB.84.075209

[4] B.K. Ismaylov, N.F. Zikrillayev, K.A. Ismailov, and Z.T. Kenzhaev, "Physical mechanism of gettering of impurity Ni atom clusters in Si lattice," Semiconductor Physics, Quantum Electronics & Optoelectronics, **27**(3), 294-297. (2024). https://doi.org/10.15407/spqeo27.03.294

[5] T. Jungwirth, J. Sinova, J. Masek, J. Kucera, and A.H. MacDonald, "Theory of ferromagnetic (III,Mn)V semiconductors," Reviews of Modern Physics, **78**(3), 809–864 (2006). https://DOI.org/10.1103/RevModPhys.78.809

[6] K.A. Ismailov, N.F. Zikrillaev, B.K. Ismaylov, Kh. Kamalov, S.B. Isamov, and Z.T. Kenzhaev, "Nickel Clusters in the Silicon Lattice," Journal of Nano and Electronic Physics, **16**(5), 05022 (2024). https://doi.org/10.21272/jnep.16(5).05022

[7] M.K. Khakkulov, A.Sh. Mavlyanov, N.A. Akbarova, and Kh. Kamalova, "Formation of Binary Compounds of Impurity Atoms of Sulfur and Zinc in Silicon," Surface Engineering and Applied Electrochemistry, **60**, 826-830 (2024). https://doi.org/10.3103/S106837552470042X

[8] Portavoce, O. Abbes, Y. Rudzevich, L. Chow, and Le Thanh, "Manganese diffusion in monocrystalline germanium," Scripta Materialia, **67**(3), 269-272 (2012). https://doi.org/10.1016/j.scriptamat.2012.04.038

[9] V. Ko, K.L. Teo, T. Liew, T.C. Chonge, M. MacKenzi, I. MacLaren, and J.N. Chapman, "Origins of ferromagnetism in transition-metal doped Si," Journal of Applied Physics, **104**(3), 033912 (2008). https://doi.org/10.1063/1.2963485

[10] X.Y. Zhang, and Z.W. Liu, "Effect of Mn diffusion on magnetic properties of Si-based diluted magnetic semiconductors," Journal of Magnetism and Magnetic Materials, **547**, 168818 (2022). https://doi.org/10.1016/j.jmmm.2021.168818

[11] S. Zhou, K. Potzger, G. Zhang, A. Mucklich, F. Eichhorn, N. Schell, R. Grotzschel, *et al.*, "Structural and magnetic properties of Mn-implanted Si," Physical Review B, **75**, 085203 (2007). https://doi.org/10.1103/PhysRevB.75.085203

[12] K.A. Ismailov, X.M. Iliev, M.O. Tursunov, and B.K. Ismaylov, "Formation of complexes consisting of impurity Mn atoms and group VI elements in the crystal lattice of silicon," Semiconductor Physics, Quantum Electronics & Optoelectronics, **24**(3), 255-260. (2021). https://doi.org/10.15407/spqeo24.03.255

[13] F. Fang, P.B. Johnson, J. Kennedy, and A. Markowitz, "Magnetic-ion-doped silicon nanostructures fabricated by ion implantation and electron beam annealing," Nuclear Instruments and Methods in Physics, **307**(10), 131–136. (2013). https://doi.org/10.1016/j.nimb.2012.11.071

[14] M.K. Bakhadyrkhanov, K.S. Ayupov, K.M. Iliev, G.K. Mavlonov, and O.E. Sattorov, "Effect of electric field, illumination, and temperature on negative magnetoresistance of low-temperature-diffusion-doped silicon," Technical Physics Letters, **36**(8), 741-744 (2010). https://doi.org/10.1134/S1063785010080195

[15] M.K. Bakhadyrkhanov, O.E. Sattarov, Kh.M. Iliev, K.S. Ayupov, and T. Umaier, "Stimulation of negative magnetoresistance by an electric field and light in silicon doped with boron and manganese," Semiconductors, **39**(7), 789–791 (2005). https://doi.org/10.1134/1.1992635

[16] M.K. Bakhadyrkhanov, G.K. Mavlonov, S.B. Isamov, and S.A. Tachilin, "Photoconductivity of silicon with multicharged clusters of manganese atoms $[Mn]_4$," Surface Engineering and Applied Electrochemistry, **46**(3), 276–280 (2010). https://doi.org/10.3103/S1068375510030154

[17] T. Dietl, H. Ohno, F. Matsukura, J. Cibert, and D. Ferrand, "Zener model description of ferromagnetism in zinc-blende magnetic semiconductors," Science, **287**(5455), 1019–1022. (2000). https://doi.org/10.1126/science.287.5455.1019

[18] S. Zhou, and H. Schmid, "Mn-doped Ge and Si: A Review of the Experimental Status," Materials, **3**(12), 5054-5082 (2010). https://doi.org/10.3390/ma3125054

[19] S. Zhou, K. Potzger, G. Zhang, *et al.*, "Structural and magnetic properties of Mn-implanted Si," January Physical Review B, **75**(8), 110-123. (2007). https://doi.org/10.1103/PhysRevB.75.085203

[20] Y.H. Kwon, T.W. Kang, H.Y. Cho, and T.W. Kim, "Formation mechanism of ferromagnetism in $Si_{1-x}Mn_x$ diluted magnetic semiconductors," Solis State Commun. **136**, 257 (2005). https://doi.org/10.1016/j.ssc.2005.08.011

[21] M.O. Tursunov, Kh.M. Iliev, and B.K. Ismaylov, "High-temperature analysis of silicon properties with manganese-oxygen binary complexes," Physical Sciences and Technology, **11**(1-2), 4-12 (2024). https://doi.org/10.26577/phst2024v11i1a1

[22] O.E. Sattarov, A. Mavlyanov, A. An, "Effect of manganese atoms on the magnetic properties of silicon," Surface Engineering and Applied Electrochemistry, **59**(2), 216-219 (2023). https://doi.org/10.3103/S106837552302014X

[23] Z.M. Saparniyazova, M.K. Bakhadyrkhanov, *et al.*, "Structural and magnetic properties of manganese-doped silicon," Inorganic Materials, **48**(4), 325–333 (2012). https://doi.org/10.1134/S0020168512030144

[24] M.K. Bakhadirkhanov, G.H. Mavlonov, X.M Iliev, O.E. Sattarov, and S.A. Tachilin, "Specific features of magnetoresistance in overcompensated manganese-doped silicon," Semiconductors, **48**(8), 986-998 (2014). https://doi.org/10.1134/S106378261408003X

[25] Sh.B. Utamuradova, A.Sh. Mavlyanov, Sh.A. Sobirova, and O.E. Sattarov, "Hybrid Secondary Structure of Manganese and Sulfur in Silicon," Surface Engineering and Applied Electrochemistry, **61**, 633-636 (2025). https://doi.org/10.3103/S1068375525700681

ФЕРОМАГНЕТИЗМ КІМНАТНОЇ ТЕМПЕРАТУРИ ТА СПІНОВА ПОЛЯРИЗАЦІЯ В КРЕМНІЇ, ЛЕГОВАНОМУ МАРГАНЦЕМ

Олмас Е. Саттаров, Бахромджон А. Абдурахманов, Гійос А. Кушієв, Станіслав А. Тачілін, Темур Б. Ісмаїлов, Забарджат Н. Умарходжаєва

Ташкентський державний технічний університет, вул. Університетська, 2, 100095, м. Ташкент, Узбекистан

У цьому дослідженні ми досліджуємо магнітні властивості кремнію, легованого марганцем, за допомогою процесу термічної дифузії. Отримані результати демонструють чіткі докази феромагнетизму при кімнатній температурі в кремнію p-типу, який виникає внаслідок вирівнювання спінів атомів Mn і наявності опосередкованої дірками провідності. Аналіз магнітоопору та гістерезису підтверджує спін-залежний транспорт, вказуючи на те, що обмінні взаємодії, опосередковані носіями, відповідають за спостережуване магнітне впорядкування. Комбінація атомно-силової мікроскопії (AFM), скануючої електронної мікроскопії (SEM) і енергодисперсійної рентгенівської спектроскопії (EDS) підтверджує успішне включення атомів Mn в решітку Si без значного пошкодження решітки. Спостережувані петлі гістерезису як при 150 K, так і при 300 K демонструють стабільну феромагнітну поведінку з коерцитивними силами 115 Oe і 87 Oe відповідно. Ці висновки відкривають багатообіцяючі перспективи для розробки спінтронних пристроїв на основі кремнію з використанням CMOS-сумісної технології термодифузії.

Ключові слова: *кремній; дифузія марганцю; феромагнетизм; нанокластери; гістерезис; спінтроніка*